ISBN: 978-3-95450-184-7 doi:10.18429/JACoW-IPAC2018-TUPAF062

PARAMETRIC STUDY OF THE BEAM FOOTPRINT CHARACTERISTICS ON THE ESS TARGET

R. Miyamoto*, ESS, Lund, Sweden
H.D. Thomsen, ISA, Aarhus University, Aarhus C, Denmark

Abstract

The beam delivery system of the ESS linac utilizes fast oscillating triangular wave dipole magnets of two transverse planes (raster magnets) to spray each long beam pulse (2.857 ms) over a rectangular cross-check pattern on the target. The characteristics of this beam footprint on the target are determined by the amplitudes of the raster magnets, RMS sizes of the beam and, in some case, the tail of the beam profile and have to satisfy the requirements from the target for the peak density as well as the fraction outside of a given rectangular boundary. This paper presents approximate closed-form expressions for the characteristics of the beam footprint and, based on the presented expressions, explores the parameter space of the raster magnets and beam parameters for achieving the optimal characteristics of the beam footprint.

INTRODUCTION

The European Spallation Source [1] will be a spallation neutron source driven by a proton linac, whose 2 GeV energy, 62.5 mA peak current, and 4% duty cycle (2.857 ms pulse length and 14 Hz repetition rate) produces an unprecedented 5 MW average power once it fulfills its full potential. Accelerator-to-Target (A2T) section [2], the final part of the linac, houses fast oscillating triangular waveform dipoles for both transverse planes (*raster system*) [3], which spray a long 2.857 ms (= T) pulse over a rectangular cross-check pattern on the target for reducing the beam density. The nominal frequencies of the raster systems are f_x = 39.55 kHz and f_y = 29.05 kHz, making numbers of oscillation periods over a single pulse f_xT = 133 and f_yT = 83 [2]. These large numbers of oscillation periods, together with the irreducible ratio of 83/133 between the two planes, make the spray pattern very dense, effectively a uniform square distribution. The A2T beam optics, consisting of six quadrupoles, also enlarges the beam RMS sizes on the target but this is rather for a protection purpose instead of beam density reduction.

Figure 1 shows a simulated current density distribution on the target. Note, following a convention of our target team, the current density in this paper is time-averaged, *i.e.,* taking into account the 4% duty cycle. We can see in Fig. 1 that the distribution has a wide flat region thanks to the rastering. The target defines two rectangular boundaries within which 99% or 99.9% of particles have to be contained [4]. These boundaries are also illustrated in Fig. 1. These requirements on the boundary are currently under a revision [5] but we follow an existing set [4] in this paper.

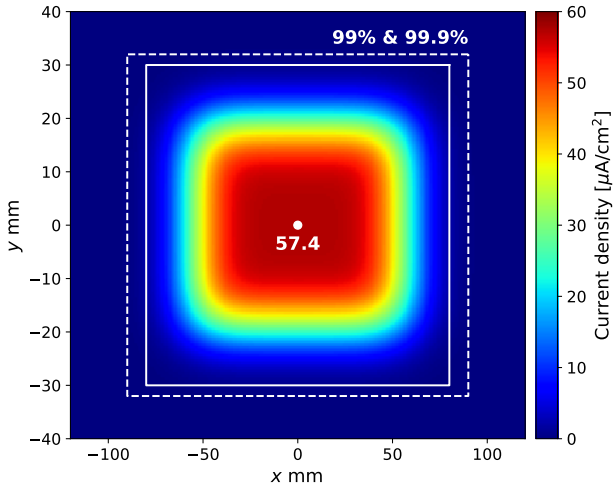

Figure 1: Simulated current density distribution on target.

Table 1 lists the beam parameters of Fig. 1, where $\sigma_{x,y}$ is the beam RMS size, $a_{x,y}$ is the rastering amplitude, and $\bar{J}_{\max}$ is the maximum current density. The product of the RMS sizes $\sigma_x \times \sigma_y$ is referred to as *beamlet size* in the following. The table also lists requirements from the target [4]. As discussed in the next section, the rastering makes the maximum current density independent of the RMS sizes, as given by $(I_b d)/(4a_x a_y)$ where I_b = 62.5 mA is the peak current and d = 4% is the duty cycle. Compared to that of the Gaussian distribution, $(I_b d)/(2\pi\sigma_x\sigma_y)$, the reduction due to the rastering for this particular case is $(\pi\sigma_x\sigma_y)/(2a_x a_y) \sim 0.1$.

In addition to the requirements on the maximum current density and the boundary, there is also an requirement on the

Table 1: Beam on Target Parameters and Requirements

Type	Parameter	Unit	Value
Beam	σ_x	mm	13.5
	σ_y	mm	5.05
	a_x	mm	56.4
	a_y	mm	19.3
	$\sigma_x\sigma_y$	mm^2	68
	$\bar{J}_{\max}$	μA/cm^2	57
	99% boundary	mm×mm	157×56
	99.9% boundary	mm×mm	180×64
Req.	$\sigma_x\sigma_y$	mm^2	> 47
	$\bar{J}_{\max}$	μA/cm^2	< 71
	99% boundary	mm×mm	< 160×60
	99.9% boundary	mm×mm	< 180×64

* ryoichi.miyamoto@esss.se

ISBN: 978-3-95450-184-7 doi:10.18429/JACoW-IPAC2018-TUPAF062

minimum beamlet size. This requirement is for protection so that the target is not damaged even if the raster system fails and the full single pulse is incident to the target. If we choose the ratio σ_y/σ_x to be identical to the ratio of the 99% boundary, this requirement defines the beam RMS sizes on the target. For the case of Table 1, the beamlet size of 68 mm^2 (with some margin with respect to the required 47 mm^2) and the y-x ratio of 60/160 (= 3/8) from the 99% boundary gives σ_x = 13.5 mm and σ_y = 5.05 mm. Once the RMS sizes are fixed, the possible maximum rastering amplitude is determined from the boundary requirements. This process to determine the rastering amplitude remains the same even for the real machine.

The requirements listed in Table 1 are not absolute but, rather, could change during the course of operations depending upon the energy and current of the linac of a given time period. Because of this situation, we developed a closed-form parametrization of the beam on target distribution, which allows a prompt calculation of the possible maximum rastering amplitude for a given RMS size and boundary requirement. The next section presents this parametrization and we conclude the paper with some studies on the beam on target characteristics utilizing this parametrization.

PARAMETRIZATION

We start from the distribution of a Gaussian bunch with an RMS size σ and offset x_0:

$$\rho_b(x, x_0) = \frac{1}{\sqrt{2\pi}\sigma} e^{-\frac{(x-x_0)^2}{2\sigma^2}} . \quad (1)$$

The distribution of the 1D projection of the rastering pattern, with an amplitude a, is uniform and given by

$$\rho_r(x_0) = \begin{cases} 1/(2a) & \text{when } |x_0| \le a \\ 0 & \text{when } |x_0| > a \end{cases} . \quad (2)$$

The 1D projection of the beam on target distribution is the convolution of $\rho_b(x, x_0)$ and $\rho_r(x_0)$ and given by

$$\rho_{\rm tot}(x) = \frac{1}{2a}\left[\frac{1}{2}\,\mathrm{erf}\left(\frac{x+a}{\sqrt{2}\sigma}\right) - \frac{1}{2}\,\mathrm{erf}\left(\frac{x-a}{\sqrt{2}\sigma}\right)\right] . \quad (3)$$

When the rastering amplitude is much larger than the RMS size ($a \gg \sigma$), like the case of ours, the distribution $\rho_{\rm tot}(x)$ has a plateau with a peak value $1/(2a)$ and crosses the half peak value at the rastering amplitude a. As already mentioned, the peak value being $1/(2a)$ makes the maximum current density $(I_b d)/(4a_x a_y)$ and independent of the RMS sizes. Figure 2 shows an example of $\rho_{\rm tot}(x)$ for the values σ_x and a_x from Table 1.

When considering the boundary requirements, we also need the cumulative distribution (from $-\infty$ to x):

$$\Phi(x) = \frac{1}{2} + \frac{x+a}{4a}\,\mathrm{erf}\left(\frac{x+a}{\sqrt{2}\sigma}\right) + \frac{\sigma}{2\sqrt{2\pi}a} e^{-\frac{(x+a)^2}{2\sigma^2}} - \frac{x-a}{4a}\,\mathrm{erf}\left(\frac{x-a}{\sqrt{2}\sigma}\right) - \frac{\sigma}{2\sqrt{2\pi}a} e^{-\frac{(x-a)^2}{2\sigma^2}} , \quad (4)$$

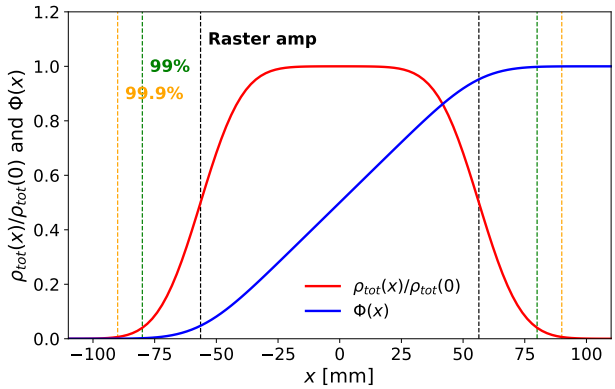

Figure 2: 1D projection of beam on target distribution.

where the following formula was used for the integration of the error function:

$$\int \mathrm{erf}(x)\,dx = x\,\mathrm{erf}(x) + \frac{1}{\sqrt{\pi}} e^{-x^2} . \quad (5)$$

Figure 2 also includes an example of $\Phi(x)$. Again, when the rastering amplitude is larger than the RMS size ($a \gg \sigma$), $\Phi(x)$ for $x > 0$ can be simplified to

$$\Phi(x) \sim 1 + \frac{x-a}{4a}\,\mathrm{erfc}\left(\frac{x-a}{\sqrt{2}\sigma}\right) - \frac{\sigma}{2\sqrt{2\pi}a} e^{-\frac{(x-a)^2}{2\sigma^2}} . \quad (6)$$

The possible maximum rastering amplitude for a given RMS size and boundary requirement is calculated by simply solving this equation for. For example, a_x = 56.4 mm in Table 1 was derived for conditions of $\Phi = (1-0.999)/4$, x = 90 mm, and σ_x = 13.5 mm. Note that Eq. 6 has the following asymptotic form but even Φ = 99.9% is not large enough to allow to truncate higher order terms. Hence, when we consider the boundary requirements of 99% or 99.9% levels, the full expression of Eq. 6 has to be numerically solved.

$$\Phi(x) \sim 1 + \frac{\sigma}{2\sqrt{2\pi}a} e^{-\frac{(x-a)^2}{2\sigma^2}} \sum_{n=1}^{\infty} (-1)^n \frac{(2n-1)!!}{2^n} \left(\frac{\sqrt{2}\sigma}{x-a}\right)^{2n} \quad (7)$$

PARAMETRIC STUDIES

This section presents two examples of parametric studies on the beam on target parameters, utilizing the parametrization developed in the previous section.

Current Density vs. Beamlet Size

If, in Table 1, the beamlet size is changed from 68 mm^2 whereas the boundary requirements for 90% and 99.9% remain the same, the possible range of the rastering amplitude for a given RMS size is given in Fig 3. The black circles corresponding to the values of Table 1. To lower the current density as possible, we adopt the maximum amplitude within the allowed range but, for the real machine, we have to take some margins taking into account accuracies of available diagnostics devices. We can also see in this figure that,

ISBN: 978-3-95450-184-7 doi:10.18429/JACoW-IPAC2018-TUPAF062

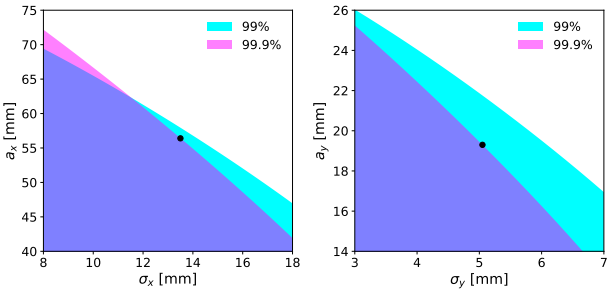

Figure 3: Rastering amplitude ranges for a given RMS size, satisfying the 99% and 99.9% boundary requirements.

in vicinity of the black circles for Table 1, the boundary requirement for 99.9% is more stringent, thus defining the limit of the rastering amplitude.

Figure 4 shows the maximum current density for a given set of RMS sizes, combining the information of two figures in Fig. 3. On the white dashed line, σ_x and σ_y have the ratio same as the 99% boundary. The black circle again represents the values of Table 1. Through gaining experiences, we may gain confidence to reduce the beamlet size and thus the current density. A benefit from the current density reduction is a longer target lifetime (nominally ~5 years). For example, if we reduce the beamlet size to the required limit of 47 mm^2, the maximum current density becomes 45 μA/cm^2. Compared to the values in Table 1, a ~30% reduction in the beamlet size provides only a ~20% reduction in the current density. This is obviously because of the rastering. The optics of A2T itself has flexibility of reducing the beamlet size, but the gain the current density reduction gets less when the beamlet size gets smaller, as nature of the rastering.

Halo on the Boundary Requirement

Our discussions thus far have assumed a bunch has an ideal Gaussian distribution. If beam halo is present, density in

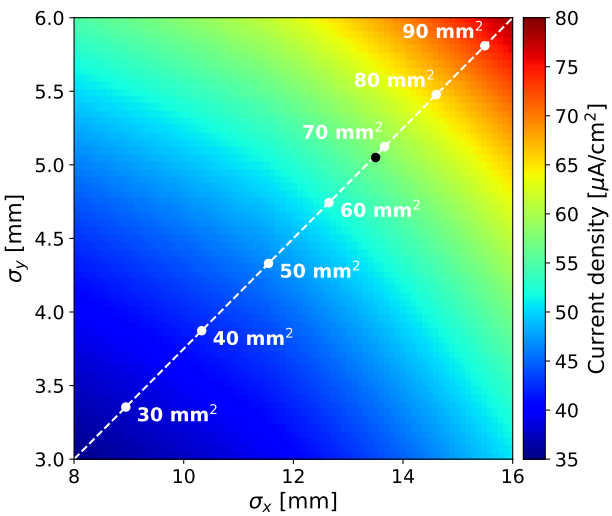

Figure 4: Maximum current density for a given set of RMS sizes. On the white dashed line, σ_x and σ_y have the same ratio as the boundary requirement for 99%.

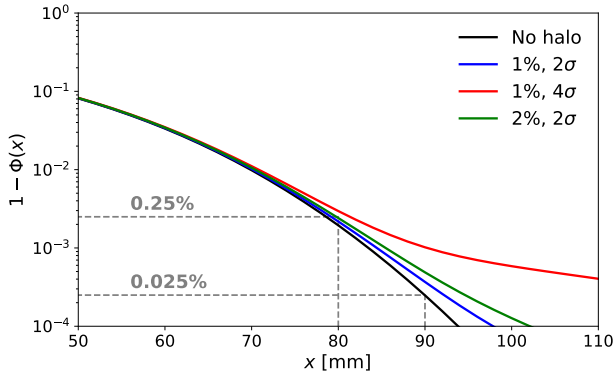

Figure 5: Impact from the double-Gaussian type halo.

the distribution tail increases and the boundary requirement is affected. An often used simple model of the halo is a secondary Gaussian distribution. For example, if a fraction δ has a RMS size of $n \times \sigma$, the distribution of a single bunch in Eq. 1 is modified to

$$\rho_b(x, x_0) = \frac{1-\delta}{\sqrt{2\pi}\sigma} e^{-\frac{(x-x_0)^2}{2\sigma^2}} + \frac{\delta}{\sqrt{2\pi}n\sigma} e^{-\frac{(x-x_0)^2}{2(n\sigma)^2}} . \quad (8)$$

When a single bunch distribution is given in this way, the total and its cumulative distribuiotn are also given as a superposition of the main and halo parts and can be easily calculated. Figure 5 shows the complimentary cumulative distribution, $1-\Phi(x)$, *i.e.,* the particle fraction beyond a given position x, for three scenarios of halo. The RMS size and amplitude were ones for the horizontal plane in Table 1 and δ and n in Eq. 8 are chosen to be δ = 1% or 2% and n = 2 or 4. Because a_x in Table 1 was determined from the boundary requirement of 99.9% (see Fig. 3), the curves are over the 99.9% boundary line as soon as the halo being introduced. If the halo indeed has a large tail as 4σ, like the case of the red curve, the rastering amplitude has to be reduced by tens of millimeters and this qualitatively demonstrates that a boundary condition for a very small fraction is sensitive to the tail distribution.

CONCLUSIONS

The raster system in the last A2T section of the ESS linac sprays the long pulse of the linac over a rectangular region on the target. A closed-form parametrization was derived for the convoluted distribution of the rastering pattern and the Gaussian distribution of each bunch. The derived parametrization allowed a prompt calculation of the possible maximum rastering amplitude for a given beam RMS size and boundary requirement. Parametric studies on characteristics of the beam on target, including the effect of the beam halo on the boundary requirement, were also presented.

ACKNOWLEDGMENT

Authors would like to thank to M. Eshraqi, Y. Lee, and T. Shae for useful discussions.

ISBN: 978-3-95450-184-7 doi:10.18429/JACoW-IPAC2018-TUPAF062

REFERENCES

[1] R. Garoby *et al.*, "The European Spallation Source Design", Phys. Scr. **93**, 014001 (2018).

[2] H.D. Thomsen and S. P. Møller, "The ESS High Eenergy Beam Transport After the 2013 Design Update", presented at IPAC'14, paper WEPRO073.

[3] H.D. Thomsen and S. P. Møller, "The Design of the Fast Raster System for the European Spallation Source", presented at IPAC'14, paper WEPRO072.

[4] E. Pitcher and T. Shea, "Beam on Target Requirements", ESS Document No. ESS-0003310, 2015.

[5] Y. Lee, H.D. Thomsen, and T. Shea, "The Beam Conditions on the Target and its Operational Impacts on Beam Intercepting Devices at European Spallation Source", presented at High Brightness Hadron Beams (2018).